Nanoscale

Cite this: *Nanoscale*, 2011, **3**, 3132

www.rsc.org/nanoscale

PAPER

In situ self-assembly of mild chemical reduction graphene for three-dimensional architectures

Wufeng Chen and Lifeng Yan*

Received 8th April 2011, Accepted 22nd April 2011
DOI: 10.1039/c1nr10355e

Three-dimensional (3D) architectures of graphene are of interest in applications in electronics, catalysis devices, and sensors. However, it is still a challenge to fabricate macroscopic all-graphene 3D architectures under mild conditions. Here, a simple method for the preparation of 3D architectures of graphene is developed *via* the *in situ* self-assembly of graphene prepared by mild chemical reduction at 95 °C under atmospheric pressure without stirring. No chemical or physical cross-linkers or high pressures are required. The reducing agents include $NaHSO_3$, Na_2S, Vitamin C, HI, and hydroquinone. Both graphene hydrogels and aerogels can be prepared by this method, and the shapes of the 3D architectures can be controlled by changing the type of reactor. The 3D architectures of graphene have low densities, high mechanical properties, thermal stability, high electrical conductivity, and high specific capacitance, which make them candidates for potential applications in supercapacitors, hydrogen storage and as supports for catalysts.

Introduction

Carbon materials consisting of three-dimensional (3D) interconnected micropores and mesopores have attracted much attention for their many desirable properties, such as being lightweight and having high porosity, large surface, and high electrical conductivity.[1] Hydrogels and aerogels are the two typical kinds of 3D carbon structures, and demonstrate potential applications in a variety of areas such as sensors,[2] supercapacitors,[3] microelectromechanical systems,[4] thermal or acoustic insulators,[5] catalytic eletrodes,[6] and environmental applications.[7,8] Recently, there have been some reports on the preparation of 3D carbon aerogels or foams based on carbon nanotubes (CNTs) due to their excellent mechanical and electronic properties.[4,9–11]

Graphene, a single sheet of carbon atoms patterned in a honeycomb lattice form, has recently attracted much attention for its unique electronic properties, excellent mechanical properties, and superior thermal properties.[12,13] Self-assembly of graphene is a simple method for the preparation of novel materials, such as one-dimensional (1D) tube-in-tube nanostructures,[14] and two-dimensional (2D) graphene films for various applications.[15–21] It is believed that developing the 3D structures of graphene will further expand its significance in applications. However, the reported methods for the preparation of 3D graphene structures are still limited, and most of them are compositions of graphene and polymers[22–26] or carbon nanotubes.[27–29] For example, Worsley *et al.* recently reported the synthesis of a graphene aerogel with high electrical conductivity ($\sim 1 \times 10^2$ S m^{-1}), and the synthesis was carried out by sol–gel polymerization of resorcinol (R) and formaldehyde (F) with sodium carbonate as a catalyst (C) in an aqueous suspension of graphene oxide (GO).[30] Ion linkages have also been applied for the preparation of 3D architectures of graphene.[31,32] However, it is still difficult to prepare 3D architectures of graphene in the absence of chemical or physical cross-linkers.[33] Shi *et al.* prepared graphene *via* a one-step hydrothermal process under high pressure, and the obtained hydrogel is electrically conductive, mechanically strong, and exhibits a high specific capacitance.[34] However, the requirement of high pressure limits its preparation on a large scale. So, it is still a challenge to prepare 3D architectures of all graphene by a mild method, especially under atmospheric pressure.

Here, we report a simple and mild method to synthesize 3D architectures of graphene *via* an *in situ* self-assembly of graphene obtained by mild chemical reduction of GO in water under atmospheric pressure. Various reducing agents have been studied for the preparation of target products, and their mechanical properties, thermal stability, electrical conductivity and specific capacitance have also been studied.

Experimental

Materials

Graphite powder, natural briquetting grade, ~100 mesh, 99.9995% (metals basis) was purchased from Alfa Aesar.

Hefei National Laboratory for Physical Sciences at the Microscale and Department of Chemical Physics, University of Science and Technology of China, Hefei, 230026, P.R. China. E-mail: lfyan@ustc.edu.cn; Fax: +86-551-3603748; Tel: +86-551-3606853

Analytical grade $NaHSO_3$, $Na_2S \cdot 9H_2O$, $NaNO_3$, $KMnO_4$, 85% $N_2H_4 \cdot H_2O$, 98% H_2SO_4, 30% H_2O_2 aqueous solution, Vitamin C, HI, and hydroquinone were purchased from Shanghai Chemical Reagents Company, and were used directly without further purification. Ultra-pure water (18 MΩ) was produced using a Millipore System (Millipore Q, USA).

Synthesis of 3D architectures of graphene

GO was prepared by a modified Hummer method.[35,36] Then, aqueous suspensions of GO at concentrations of 0.1–2.0 mg ml^{-1} were prepared, and various reducing agents such as $NaHSO_2$, Na_2S, Vitamin C, HI, or hydroquinone (27–54 mmol L^{-1}) were added. The mixed suspension was heated at 95 °C for 30 min or 3 h without stirring. Then, the as-prepared graphene hydrogel was dialyzed against deionized water for 3 days to remove residual inorganic compounds. For aerogel preparation, the as-prepared graphene hydrogel was freeze-dried to remove absorbed water.

Characterization of the 3D architectures of graphene

The morphologies of the hydrogels and aerogels were characterized by SEM (Superscan SSX-550, Shimazu). The thermal properties of the samples were recorded by a thermogravimeter (TGA, DTA-50, Shimazu), and all of the measurements were carried out under nitrogen gas over a temperature range of 30–800 °C with a ramp rate of 5 °C min^{-1}. Wide-angle X-ray diffraction (XRD) analyses were carried out on an X-ray diffractometer (D/MAX-1200, Rigaku Denki Co. Ltd., Japan). Elemental analysis was carried out using a VARIO ELIII analyzer (Elemental analysis system Co. Ltd., Germany). The electrical conductivities of samples were measured using a two-probe method with a Kelthley-4200 instrument. TEM images were obtained on a Hitachi H-800 microscope at 200 kV.

Electrochemical measurement of graphene hydrogel based supercapacitor

Slices of graphene hydrogel (1 mm in thickness) were used as electrodes for the supercapacitor, with 5 M aqueous KOH solution as the electrolyte, while Pt foils were used as the current collector. Cyclic voltammetry (CV) and galvanostatic charge/discharge experiments were performed on a CHI660C potentiostat-galvanostat (CH Instruments Inc.)

Results and discussion

GO is hydrophilic and can be well dispersed into water to form a stable suspension, and the reduction of GO by $NaHSO_3$ in an aqueous suspension under mild conditions could result in the formation of hydrophobic graphene.[37] It is well-known that the final products should be aggregates or precipitates if the reduction is carried out under stirring, and the aggregates or precipitates are believed to be formed from the crude self-assembly of the as-formed graphene due to the increase in its hydrophobicity. What will happen if the self-assembly occurs free of disturbance? The possibility of the stacking of the reduced graphene which retains its orientation may increase, due to the steric hindrance effect of the graphene sheets with sizes of micrometres. As a result, an efficient self-assembly may occur, driven by the hydrophobic and π–π

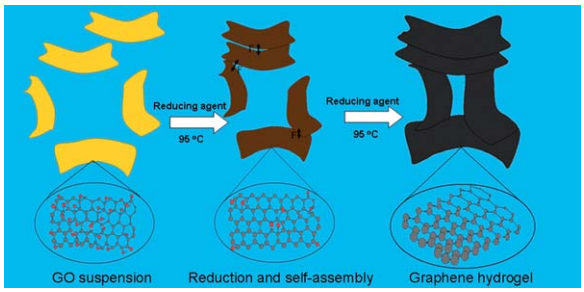

Scheme 1 The proposed self-assembly mechanism for graphene hydrogel formation during the chemical reduction of GO in an aqueous suspension.

stacking interactions of the conjugated structures of graphene, and a 3D architecture of graphene may be formed, as shown in Scheme 1. At the early stage of reduction, some sheets of partially reduced graphene oxide appear, and their increasing hydrophobicity leads to aggregation. Some sheets of reduced graphene oxide assemble together in parallel, but others may assemble at any angle. At the end, much water was expelled out from the aggregates and compact 3D architectures could be formed.

In our studies, $NaHSO_3$ (41 mmol L^{-1}) was selected as reducing agent at first for the reduction of GO in aqueous

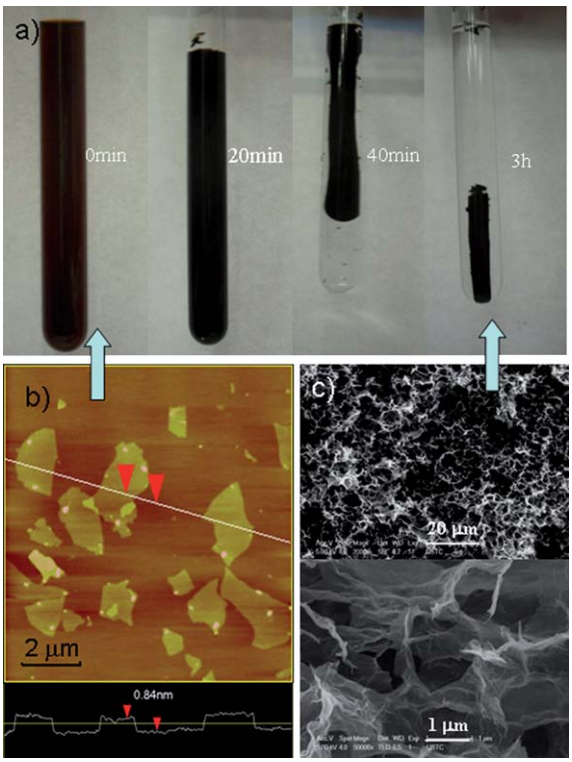

Fig. 1 The preparation and structure of a graphene hydrogel. a) The formation process of the graphene hydrogel from an aqueous GO suspension (1.5 mg ml^{-1}) *via* a one-step self-assembly of graphene from *in situ* reduction of GO fordifferent times using $NaHSO_3$ (41 mmol L^{-1}) as reducing agent. b) An AFM height image of the GO aqueous suspension deposited onto the surface of newly cleaved mica. c) SEM cross-section images of the as-prepared graphene hydrogel (3 h) at different magnifications.

suspensions, which was prepared as the well-known Hummers method.[35] The reaction was carried out at 95 °C under atmospheric pressure without stirring. Fig. 1 shows the changes of the reactive system *versus* reaction time. Clearly, an *in situ* self-assembly of the as-formed graphene sheets occurs. Before reduction, GO can be well dispersed in water to form a stable aqueous suspension (1.5 mg ml^{-1}), as shown in Fig. 1a (0 min). Fig. 1b shows a typical atomic force microscopy (AFM) height image of GO sheets on the surface of newly cleaved mica, and the as-prepared GO is in a single layer with height of about 0.84 nm. The photographs of the reaction system at reaction times of 20, 40 and 180 min are also shown in Fig.1a. Apparently, after a reduction reaction of 20 min, the aqueous suspension of GO turned dark and remained homogeneous, indicating the partial reduction of GO. However, after reaction for 40 min, a rod-shaped aggregate was formed, which floated on the top of the suspension. In addition, the bottom of the tube became clear, and the shrinkage of the dark region indicates the self-assembly of graphene obtained from the *in situ* reduction of GO. Continuously, a small rod was formed at the end of the reduction (180 min), and its density was greater than that of water and it sank to the bottom of the tube. The rod was hydrophilic and still retained some water inside which could be squeezed out by pressing, and a graphene hydrogel was prepared. Fig. 1c shows SEM images of its cross-section at different magnifications. Clearly, the as-prepared material has a 3D architecture with homogeneously interconnected pores with sizes of 1–2 micrometres. In addition, the walls of the pores are thin, indicating that the overlap of the graphene layers is not so high. An elemental analysis study showed that the ratio of C/O in the as-prepared graphene hydrogel was 7 : 1, indicating an efficient reduction of GO.

Fig. 2 shows the X-ray diffraction (XRD) patterns of pristine graphite, GO, and the as-prepared graphene hydrogel after reduction for 40 min and 180 min. For pristine graphite, the peak at 26.5° of 2θ corresponds to the (002) diffraction line with an interlayer spacing along the *c*-axis of 0.34 nm. However, for GO the peak disappeared and a wide diffraction peak appeared at 10.4°, corresponding to a *d*-spacing of 0.83 nm. After chemical reduction for 40 min, the fact that nearly all of the peaks disappeared indicates the efficient exfoliation of the multilayer during the chemical reduction of GO. However, at the end of the reduction (180 min), a new wide diffraction peak appeared at 23.5°, corresponding to an interlayer spacing of 0.38 nm. Apparently, self-assembly of the as-formed graphene occurred, which resulted in the formation of the wall of the hydrogel. The shoulder peak appearing at 43.1° is a fingerprint peak for graphite, due to the (100) diffraction, indicating the reformation of graphitic microcrystals on the graphene plane due to the chemical reduction of graphene oxide.[38]

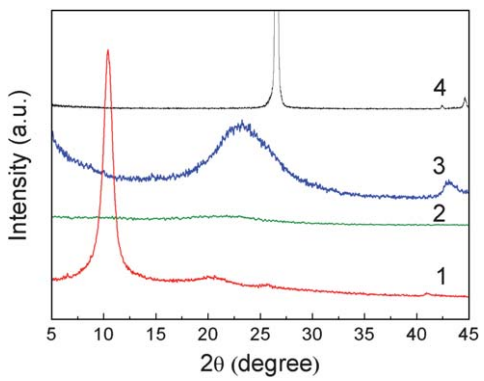

Fig. 2 XRD patterns of pristine graphite (curve 4), GO (curve 1), and 3D architectures of graphene at various reducing time of 40 min (curve 2) and 3 h (curve 3).

The as-prepared 3D architecture of graphene is a hydrogel with plenty of water remaining inside. It is well-known that aerogels could be prepared by subjecting a wet-gel precursor to freeze-drying or supercritical drying. Aerogels are ultralight, highly porous materials which have a wide range of potential applications. Here, the as-prepared graphene hydrogel was treated by freeze drying and a black graphene aerogel could be obtained. The density of the obtained graphene aerogel is 18 mg cm^{-3}. Fig. 3 shows a photograph of the as-prepared graphene aerogel and an SEM image of its cross-section, and the sizes of the pores are about 3–6 micrometres.

Fig. 4a shows typical Raman spectra of GO and a graphene aerogel prepared using $NaHSO_3$ as the reducing agent. Both of the spectra show the existence of the D, G, and 2D bands. For GO, the G band is located at 1602 cm^{-1}, while for the graphene aerogel, the G band moved to 1593 cm^{-1}, which is close to the value of the pristine graphite, and confirms the reduction of GO during the chemical treatment. However, the existence of the D band at 1355 and 1350 cm^{-1}, corresponding to GO and graphene aerogel, also predicts the defect of the sample.[37]

XPS measurements could provide direct evidence of the reduction of GO. Fig. 4b shows the C_{1s} XPS spectra of the as-prepared graphene aerogel reduced by $NaHSO_3$. The curves were fitted considering the following contributions: C=C (sp^2; peak 1), C–C (sp^3; peak 2), C–O/C–O–C (hydroxyl and epoxy groups; peak 3), C=O (carbonyl groups; peak 4), O–C=O (carboxyl groups; peak 5).[39] After the chemical reduction, the oxygen species of C–O (hydroxyl and epoxy, 286.5 eV), C=O (carbonyl, 287.9 eV) and O=C–O (carboxyl, 289.2 eV) reduced significantly, which indicates an efficient deoxidization. The major remaining species were C=C (284.6 eV) and C–C (285.6 eV).

The thermal stability of the graphene aerogels has been studied by TGA measurements. Fig. 4c shows the TG curves for GO, the as-prepared graphene aerogel, and the aerogel after annealing at 400 °C. For GO, there are two steps for mass loss on increasing the temperature. The mass loss is about 10% at around 100 °C, which can be ascribed to the removal of adsorbed water. The mass loss at around 200 °C is about 25%, attributed to the decomposition of labile oxygen functional groups.[36] For the

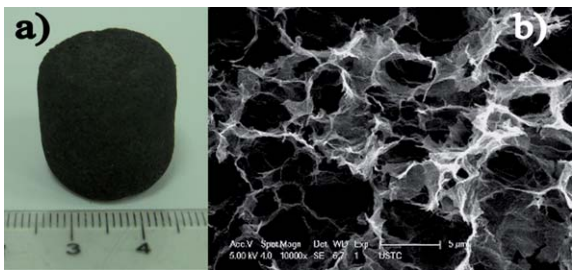

Fig. 3 A photograph of a graphene aerogel (a) and its cross-section SEM image (b).

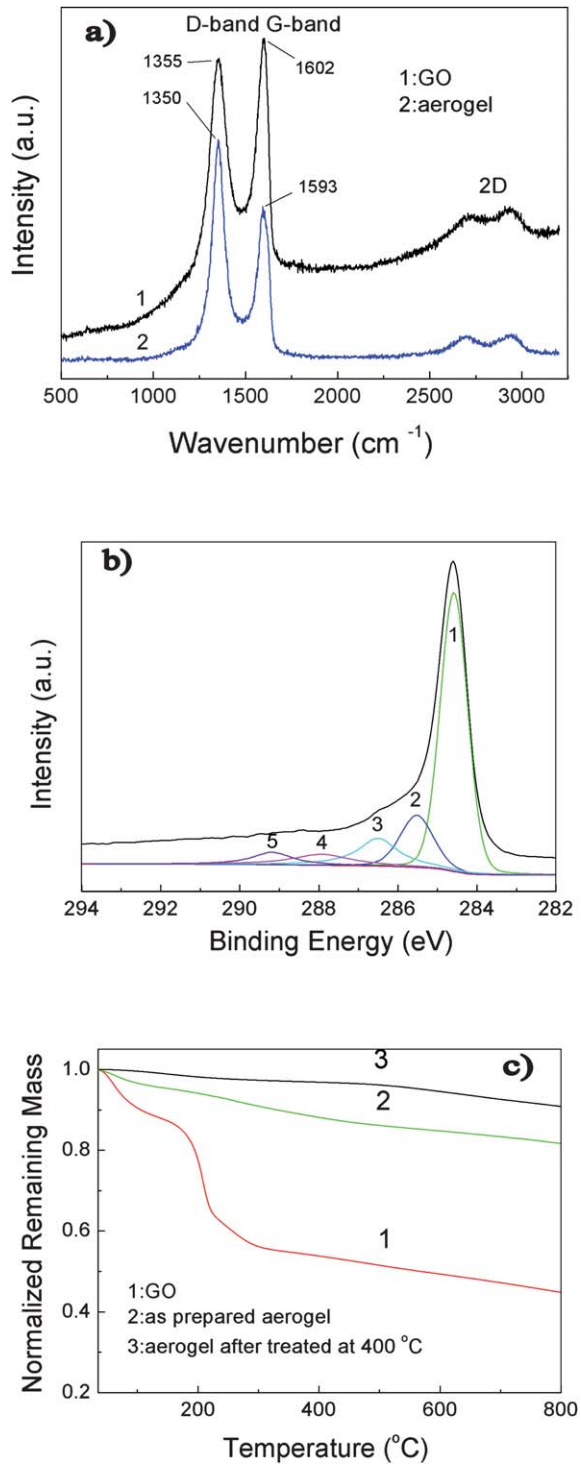

Fig. 4 a) Raman spectra of GO, the prepared graphene aerogel and the dried gel rod. b) High-resolution C1s XPS spectra of the as-prepared graphene aerogel using $NaHSO_3$ as reducing agent. c) Normalized remaining mass of GO, the as-prepared graphene aerogel and the aerogel after heating at 400 °C for 5h.

as-prepared aerogel, the mass loss is only 10% over the range 100–800 °C, indicating an efficient reduction of GO. For the aerogel after annealing at 400 °C, the mass loss is only 5% before 800 °C, indicating that the obtained graphene aerogel is thermally stable.

The mechanical properties of the as-prepared graphene hydrogel are also high. Fig. 5 shows the uniaxial compression tests of the graphene hydrogel at different set strains. The curve shows an initial linear region at $\varepsilon < 10\%$, and a plateau with gradually increasing slope until very high strains up to 60%. The elastic modulus and yield stress of the graphene hydrogel were measured to be about 0.13 MPa and 28 KPa, respectively. Fig. 5 also shows a photograph of a hydrogel supporting a mass of 200 g. Some water was extruded under the weight, but it did not break. The mechanical properties of the graphene hydrogel are comparable to those of chemically cross-linked polymer hydrogels.[40]

The graphene aerogel is a good conductor, with a measured bulk electrical conductivity of 87 S m^{-1} (aerogel density: 15 mg cm^{-3}). This value is more than 2 orders of magnitude greater than those reported for macroscopic 3D graphene networks prepared with physical crosslinks,[31,34] and is similar to a graphene aerogel prepared by organic sol–gel chemistry combined with pyrolysis.[30]

The as-prepared graphene hydrogel could be used as the electrodes of a supercapacitor without using a binding agent. Fig. 6 shows the cyclic voltammograms (CV) of a graphene hydrogel based supercapacitor at different scan rates of 10 and 20 mV s^{-1}, and both of the curves are nearly rectangular in shape, indicating nearly ideal double layer capacitance behavior of the electrode material, while the little variance from the rectangular shape could be caused by the electrode resistivity.[41] The calculated specific capacitances of the graphene hydrogel are 166 and 156 F g^{-1} at potential scan rates of 10 and 20 mV s^{-1}, respectively. The values are similar to a graphene hydrogel prepared by a hydrothermal method,[34] indicating a high specific capacitance.

Interestingly, it was found that the shape of the as-prepared graphene hydrogel is reactor-dependent. As shown in Fig. 7, various shapes of graphene hydrogels such as taper-like, cylindrical, pear-shaped, and spherical can be prepared when the relative shape of reactor was utilized. This indicates that the shrinkage of the as-formed hydrogel during the self-assembly is isotropic, and it provides a chance to prepare shape-controlled graphene hydrogels as desired.

Various kinds of reducing agent have been studied for the synthesis of graphene hydrogels. Fig. 8 shows photographs of as-prepared graphene hydrogels using Na_2S, Vitamin C, HI, and hydroquinone. It was also found that the required time for

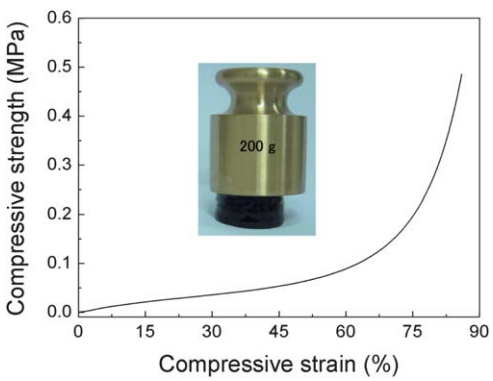

Fig. 5 A compressive stress-strain curve of the graphene hydrogel at different set strains. Inset is a photograph of the graphene hydrogel (in its wet state) supporting a 200 g weight.

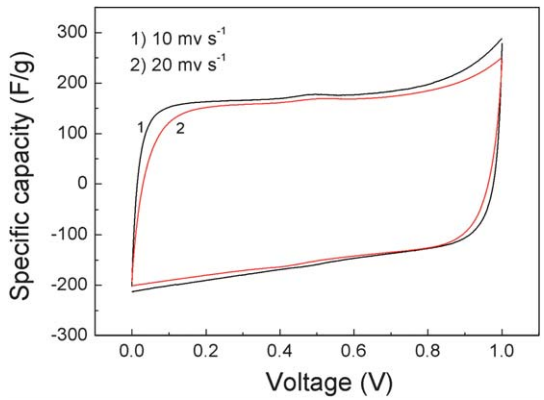

Fig. 6 Cyclic voltammograms of a graphene hydrogel based supercapacitor at two different scan rates.

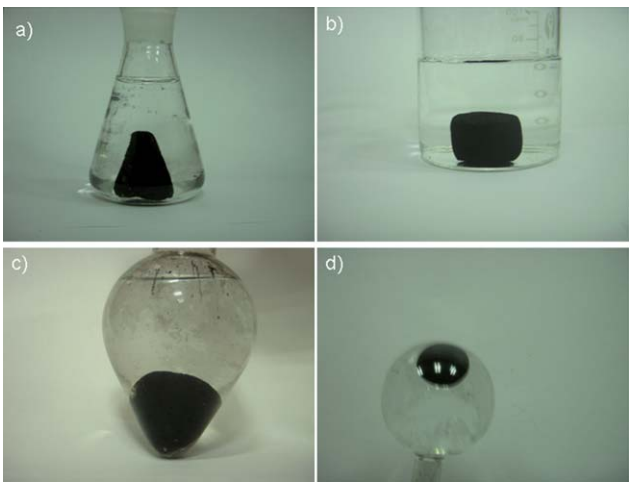

Fig. 7 The shape controlled synthesis of hydrogels using reactors of various shapes.

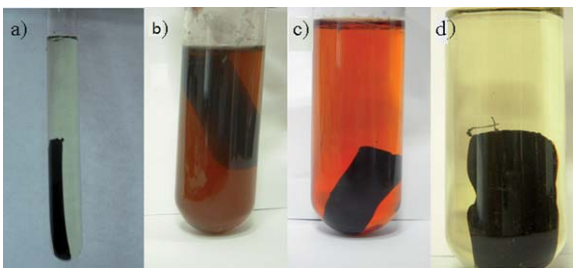

Fig. 8 Photographs of graphene hydrogels prepared using various chemical reducing agents. a) Na_2S. b) Vitamin C. c) HI, and d) hydroquinone. (GO: 1.5 mg ml^{-1}, reducing agent concentration: 41 mmol L^{-1}).

hydrogel formation is different. For example, it takes 30 min for $NaHSO_3$ while it requires only 10 min for Vitamin C and Na_2S (GO: 1.5 mg ml^{-1}, reducing agent concentration: 41 mmol L^{-1}). Interestingly, when the well-known reducing agent hydrazine was used, no 3D architecture formed at all, and the reason for this maybe that the residual nitrogen prevents the formation of the superstructure, and the details of this should be studied next. The electrical conductivities of the graphene aerogels prepared using various reducing agents were measured and the results are listed in Table 1. It can be observed that the electrical conductivity of the hydrogel prepared using HI is the highest, at110 S m^{-1}. In addition, the densities and the ratios of C/O of the products were measured, and it seems that the density and degree of reduction are the key factors for the electrical conductivity.

Table 1 The effect of various reducing agents on the properties of the as-prepared 3D architectures of graphene

Chemical reducing agents	Vitamin C	Na_2S	HI[a]	$NaHSO_3$[b]	$NaHSO_3$[c]
Electrical Conductivity (S m^{-1})	23	6.8	110	17	87
Density (mg cm^{-3})	21	15	37	18	15
Element analysis C/O	6.8	5.8	8.5	7.0	10.1

[a] HI in 80% (v/v) acetic acid aqueous solution. [b] The as-prepared graphene aerogel. [c] The graphene aerogel after it was treated at 400 °C for 5 h under vacuum for oxygen removal.

Conclusions

In summary, we have prepared 3D architectures of graphene *via* a one-step mild chemical reduction and an *in situ* self-assembly. The process is carried out under atmospheric pressure in an open system, which makes it possible to prepare 3D architectures of graphene on a large scale. Both macroscopic graphene hydrogels and aerogels could be obtained by the method. The as-prepared 3D architectures of graphene are homogenous. They also show high mechanical strength, low-density, thermal stability, high electrical conductivity, and high specific capacitance. The as-prepared 3D architectures of graphene have potential applications in supercapacitors, hydrogen storage and as supports for catalysts.

Notes and references

1 Y. S. Tao, M. Endo and K. Kaneko, *J. Am. Chem. Soc.*, 2009, **131**, 904–905.
2 X. C. Gui, A. Y. Cao, J. Q. Wei, H. B. Li, Y. Jia, Z. Li, L. L. Fan, K. L. Wang, H. W. Zhu and D. H. Wu, *ACS Nano*, 2010, **4**, 2320–2326.
3 D. N. Futaba, K. Hata, T. Yamada, T. Hiraoka, Y. Hayamizu, Y. Kakudate, O. Tanaike, H. Hatori, M. Yumura and S. Iijima, *Nat. Mater.*, 2006, **5**, 987–994.
4 M. A. Worsley, S. O. Kucheyev, J. H. Satcher, A. V. Hamza and T. F. Baumann, *Appl. Phys. Lett.*, 2009, **94**, 073115.
5 J. Wang and M. W. Ellsworth, in *Graphene and Emerging Materials for Post-Cmos Applications*, ed. Y. Obeng, S. DeGendt, P. Srinivasan, D. Misra, H. Iwai, Z. Karim, D. W. Hess and H. Grebel, 2009, pp. 241–247.
6 J. E. Trancik, S. C. Barton and J. Hone, *Nano Lett.*, 2008, **8**, 982–987.
7 M. A. Shannon, P. W. Bohn, M. Elimelech, J. G. Georgiadis, B. J. Marinas and A. M. Mayes, *Nature*, 2008, **452**, 301–310.
8 X. C. Gui, J. Q. Wei, K. L. Wang, A. Y. Cao, H. W. Zhu, Y. Jia, Q. K. Shu and D. H. Wu, *Adv. Mater.*, 2010, **22**, 617–621.
9 S. H. Lee, J. S. Park, B. K. Lim, C. Bin Mo, W. J. Lee, J. M. Lee, S. H. Hong and S. O. Kim, *Soft Matter*, 2009, **5**, 2343–2346.
10 M. D. Gawryla, L. Liu, J. C. Grunlan and D. A. Schiraldi, *Macromol. Rapid Commun.*, 2009, **30**, 1669–1673.
11 M. B. Bryning, D. E. Milkie, M. F. Islam, L. A. Hough, J. M. Kikkawa and A. G. Yodh, *Adv. Mater.*, 2007, **19**, 661–664.
12 K. S. Novoselov, A. K. Geim, S. V. Morozov, D. Jiang, Y. Zhang, S. V. Dubonos, I. V. Grigorieva and A. A. Firsov, *Science*, 2004, **306**, 666–669.
13 A. K. Geim, *Science*, 2009, **324**, 1530–1534.

14 Z. P. Zhu, D. S. Su, G. Weinberg and R. Schlogl, *Nano Lett.*, 2004, **4**, 2255–2259.
15 Z. Tang, J. Zhuang and X. Wang, *Langmuir*, 2010, **26**, 9045–9049.
16 B. G. Choi, H. Park, T. J. Park, M. H. Yang, J. S. Kim, S.-Y. Jang, N. S. Heo, S. Y. Lee, J. Kong and W. H. Hong, *ACS Nano*, 2010, **4**, 2910–2918.
17 H. L. Wang, X. R. Wang, X. L. Li and H. J. Dai, *Nano Res.*, 2009, **2**, 336–342.
18 Z. Y. Yin, S. Y. Sun, T. Salim, S. X. Wu, X. A. Huang, Q. Y. He, Y. M. Lam and H. Zhang, *ACS Nano*, 2010, **4**, 5263–5268.
19 B. Li, X. H. Cao, H. G. Ong, J. W. Cheah, X. Z. Zhou, Z. Y. Yin, H. Li, J. L. Wang, F. Boey, W. Huang and H. Zhang, *Adv. Mater.*, 2010, **22**, 3058–3061.
20 Q. Y. He, H. G. Sudibya, Z. Y. Yin, S. X. Wu, H. Li, F. Boey, W. Huang, P. Chen and H. Zhang, *ACS Nano*, 2010, **4**, 3201–3208.
21 Z. Y. Yin, S. X. Wu, X. Z. Zhou, X. Huang, Q. C. Zhang, F. Boey and H. Zhang, *Small*, 2010, **6**, 307–312.
22 H. Bai, C. Li, X. L. Wang and G. Q. Shi, *Chem. Commun.*, 2010, **46**, 2376–2378.
23 S. Z. Zu and B. H. Han, *J. Phys. Chem. C*, 2009, **113**, 13651–13657.
24 A. Satti, P. Larpent and Y. Gun'ko, *Carbon*, 2010, **48**, 3376–3381.
25 X. Y. Qi, K. Y. Pu, H. Li, X. Z. Zhou, S. X. Wu, Q. L. Fan, B. Liu, F. Boey, W. Huang and H. Zhang, *Angew. Chem., Int. Ed.*, 2010, **49**, 9426–9429.
26 X. Y. Qi, K. Y. Pu, X. Z. Zhou, H. Li, B. Liu, F. Boey, W. Huang and H. Zhang, *Small*, 2010, **6**, 663–669.
27 D. S. Yu and L. M. Dai, *J. Phys. Chem. Lett.*, 2010, **1**, 467–470.
28 L. He, J. Q. Lu and H. Q. Jiang, *Small*, 2009, **5**, 2802–2806.
29 X. Cao, Q. He, W. Shi, B. Li, Z. Zeng, Y. Shi, Q. Yan and H. Zhang, *Small*, 2011, **7**, 1199.
30 M. A. Worsley, P. J. Pauzauskie, T. Y. Olson, J. Biener, J. H. Satcher and T. F. Baumann, *J. Am. Chem. Soc.*, 2010, **132**, 14067–14069.
31 Z. H. Tang, S. L. Shen, J. Zhuang and X. Wang, *Angew. Chem., Int. Ed.*, 2010, **49**, 4603–4607.
32 X. Jiang, Y. Ma, J. Li, Q. Fan and W. Huang, *J. Phys. Chem. C*, 2010, **114**, 22462.
33 F. Liu and T. S. Seo, *Adv. Funct. Mater.*, 2010, **20**, 1930–1936.
34 Y. X. Xu, K. X. Sheng, C. Li and G. Q. Shi, *ACS Nano*, 2010, **4**, 4324–4330.
35 W. Hummers and R. Offema, *J. Am. Chem. Soc.*, 1958, **80**, 1339.
36 W. F. Chen, L. F. Yan and P. R. Bangal, *Carbon*, 2010, **48**, 1146–1152.
37 W. Chen, L. Yan and P. R. Bangal, *J. Phys. Chem. C*, 2010, **114**, 19885–19890.
38 B. Zhang, T. H. Wang, S. L. Liu, S. H. Zhang, J. S. Qiu, Z. G. Chen and H. M. Cheng, *Microporous Mesoporous Mater.*, 2006, **96**, 79–83.
39 S. Hyeon-Jin, K. Ki Kang, A. Benayad, Y. Seon-Mi, P. Hyeon Ki, J. In-Sun, J. Mei Hua, J. Hae-Kyung, K. Jong Min, C. Jae-Young and L. Young Hee, *Adv. Funct. Mater.*, 2009, **19**, 1987–1992.
40 S. E. Grieshaber, A. J. E. Farran, S. Lin-Gibson, K. L. Kiick and X. Jia, *Macromolecules*, 2009, **42**, 2532–2541.
41 E. Frackowiak and F. Beguin, *Carbon*, 2001, **39**, 937–950.